# Four-Dimensional Fuel-Optimal Guidance in the Presence of Winds

Abhijit Chakravarty*
*Boeing Commercial Airplane Company, Seattle, Washington*

**The generation of optimal trajectories from cruise altitude to 10,000 ft for a typical commercial jet transport shows that the optimal absorption of delay in arrival time requires speed reduction in conjunction with altitude excursion (the latter not attempted before). Multiple regression methods are used to develop drag and fuel flow models which are smoother and more compact than those of any previous investigation. The concept of optimal cruise descent is introduced and optimal results are compared with suboptimal strategies of constant Mach number/Calibrated Airspeed (CAS) descent and constant flight path angle descent. Finally, wind effects are analyzed, and the cost of delay as a function of wind condition is presented, followed by the effects of wind on the constant flight path angle descent.**

## Introduction

ONBOARD guidance and control systems are used to monitor and control flight performance. They also maintain updated estimates of fuel reserve and time of arrival. Presently, overall flight planning, including estimated time of arrival, is performed on ground dispatch computers. The significance of sophisticated preflight planning is reduced, however, when an aircraft wastes fuel during holds for unforecast delays. However, if the reassigned arrival time is available earlier in the flight, a fuel-optimal trajectory can be generated on-line with changed speed commands and altitude excursions that will facilitate arrival at the new time. This strategy provides considerable savings potential over the conventional "hold" strategy. It is therefore safe to conjecture that accurate control of arrival time (four-dimensional control) will play an important role in the future Air Traffic Control (ATC) system.

Digital computer technology is available which can generate optimum flight paths that minimize direct operating cost (DOC) for free terminal time. A list of pertinent references is given in Ref. 1. However, this technology lacks an efficient procedure to compute the appropriate cost of time to arrive at the assigned time of arrival. Sorensen and Waters[2] were among the first to include control of time of arrival in an extension of Erzberger's energy-state approximation.[3] They recognized the need to have smooth numerical models of drag and thrust characteristics to avoid discontinuities in the relationship of cost index to the time of arrival. Burrows[4] developed such models by using bicubic spline drag polar fits. These were used successfully to smooth climb speed commands and avoid unacceptable throttle variations during economy cruise. In this paper, however, drag and fuel flow models will be used, which have been developed using multiple regression methods, a procedure never attempted by previous investigators. The elegance and compactness of these models are attractive and the models are sufficiently smooth to avoid the predicted arrival time discontinuities.

As is well known, the general system of differential equations of motion commonly employed for aircraft trajectory computations in the longitudinal plane is fifth order and nonlinear. Thus, if the optimal control problem is formulated using Pontryagin's minimum principle, a ten-order, two point boundary value problem (TPBVP) results. A TPBVP of this order presents formidable difficulties due to the computational burden as well as numerical ill-conditioning. Consequently, considerable effort has been expended in searching for simplification techniques to produce results which are meaningful and attainable at reasonable cost.

From the research of the last decade, singular perturbation theory has emerged as the most promising approach to meet the simplification goal. With this theory, the system dynamics are separated into slow and fast modes and the solution of a higher-order problem is approximated by the solution of a series of lower-order problems. The procedure has been applied to the F-4 trajectory optimization problem by Calise[5] and Mehra et al.[6] These investigators, however, did not include the aircraft weight variation in the system formulation. However, when the weight variation is included and a transport aircraft is analyzed for time scale separation, only two distinct time scales are observed.[1] This resulting formulation still requires solution of two point boundary value problems in the inner region[7] (climb and descent segments of the trajectory). To mitigate the problem, singular perturbation theory is used in conjunction with the energy-state approximation,[8] so that the inner region now has only one state equation. This facilitates analyzing the problem using a Fibonacci search parameter optimization scheme, which reduces the computational burden sufficiently in terms of time and storage to allow real-time implementation of the algorithm.

In this paper, the use of "matched asymptotic expansions"[9] and the energy state approximation to develop a real-time algorithm for a fuel-optimal aircraft trajectory for fixed terminal time is investigated. Although the fuel savings are proportional to how long in advance the arrival time is known, only the last segment of the flight trajectory is considered. A typical example is to find an optimal trajectory from a point at cruise altitude, called the entry fix, to a point at lower altitude at which the arrival time is assigned, called the metering fix. The fuel consumption rates for two different weights and a few cost indices are delineated and the critical cost index for maximum endurance cruise is expressed as a function of weight. The concept of optimal cruise-descent is introduced and the cost of delay for different wind conditions is investigated, both for the first time. A typical example

Submitted Aug. 2, 1983; presented as Paper 83-2242 at the AIAA Guidance and Control Conference, Gatlinburg, Tenn., Aug. 15-17, 1983; revision received Oct. 31, 1983. 

*Senior Specialist Engineer, Flight Systems Research Unit. Member AIAA.

showing the convergence of cost-of-time iteration is presented, followed by comparisons with constant flight path angle descents and with standard descents with constant Machs number—constant CAS segments.

## Mathematical Formulation

### Aircraft Equations of Motion

The aircraft model used assumes a point mass approximation, that is, state variables describing the vehicle attitude are either omitted or used as control variables. The energy-state approximation of the point-mass longitudinal model of the aircraft, in the presence of wind, is taken to be in conventional state variables as follows:

$$\frac{dx}{dt} = (V + V_w) \tag{1}$$

$$\frac{dm}{dt} = -f \tag{2}$$

$$\epsilon \frac{dE}{dt} = \frac{(V + V_w)(T - D)}{mg} - V_w \gamma \tag{3}$$

where $x$ is the range, $V$ the airspeed, $V_w$ the windspeed, $m$ the mass, $f$ the fuel flow rate, $E$ the energy height, $\gamma$ the flight path angle, $T$ the thrust, and $D$ the drag. The second term on the right side of Eq. (3) is normally small and can usually be neglected. $\epsilon$ is a small "singular perturbation" parameter that arises as a consequence of the particular aircraft dynamics and an appropriate choice of scaling the equations of motion. The energy height $E$ is related to the altitude and the groundspeed through

$$E = h + (V + V_w)^2 / 2g \tag{4}$$

The airspeed $V$ and the thrust $T$ are the control variables, varying within the limits:

$$T_{\min} \le T \le T_{\max} \tag{5}$$

$$V_{\min} \le V \le V_{\max} \tag{6}$$

Both $V_{\min}$ and $V_{\max}$ are functions of altitude and represent the controllability and structural limitations on the aircraft. The airplane model also involves the fuel flow rate $f(h,M,T)$, the drag polar $C_D(C_L,M)$, and minimum and maximum thrusts $T_{\min}(M,h)$, $T_{\max}(M,h)$, which are modelled using multiple regression methods. $M$ denotes the Mach number, $C_D$ the drag coefficient, and $C_L$ the lift coefficient.

### Performance Index

The optimization problem is to steer the system, Eqs. (1)-(3) from an initial state $(x_i,m_i,E_i)$ at $t_i$ to a final state $(x_f,m_f,E_f)$ at fixed final time $t_f$ so that the fuel spent is minimized. Equivalently, minimize

$$J = \int_{t_i}^{t_f} C_f f \, dt \tag{7}$$

where $C_f$ is the cost of fuel.

### Pontryagin's Minimum Principle

The Hamiltonian for Eq. (1)-(3) and (7) is

$$H_I = C_f f + \lambda_x (V + V_w) - \lambda_m f + \lambda_E (V + V_w)(T - D)/mg \tag{8}$$

where $\lambda_x$, $\lambda_m$, and $\lambda_E$ are the range, mass, and energy adjoint variables, respectively. Pontryagin's minimum principle[10] states that the Hamiltonian is minimum along an optimal trajectory. Furthermore, since the final time is fixed, and $H_I$ is not an explicit function of time, $H_I$ is constant along the optimal trajectory and given by

$$\min_{T,V} (H_I) = K \tag{9}$$

$K$ has the units of cost per unit time, and if we select $C_t = -K$, Eq. (9) may be rewritten

$$\min_{T,V} [C_t + (C_f - \lambda_m) f + \lambda_x (V + V_w) + \lambda_E (V + V_w)(T - D)/mg] = 0 \tag{10}$$

along the optimal trajectory. It therefore reduces to a direct operating cost (DOC) optimization problem with free terminal time and cost parameters $C_f$ and $C_t$. The balance between fuel and time costs may be expressed by the so-called cost index

$$CI = \frac{C_t}{C_f} \tag{11}$$

The traditional units used in the cost index are $C_t$ in dollars per hour and $C_f$ in cents per pound. The 4-D optimization problem is now reduced to finding the correct $C_t$ or $CI$, for assigned arrival time $t_f$. If the nominal trajectory corresponds to maximum range cruise (MRC), for which $C_t = 0$, a fuel-optimal trajectory for any delay will correspond to a negative cost of time, contrary to usual DOC choices.

### Cruise Cost Function

As $\epsilon \to 0$, the outer solution (according to singular perturbation theory) is reduced to

$$\min_{\substack{h,V \\ (T=D)}} [C_t + (C_f - \lambda_m) f + \lambda_x (V + V_w)] = 0 \tag{12}$$

Using Pontryagin's minimum principle, we further get

$$-\lambda_x = \min_{h,V} \left[ \frac{C_t + (C_f - \lambda_m) f}{(V + V_w)} \right]_{T=D} \tag{13}$$

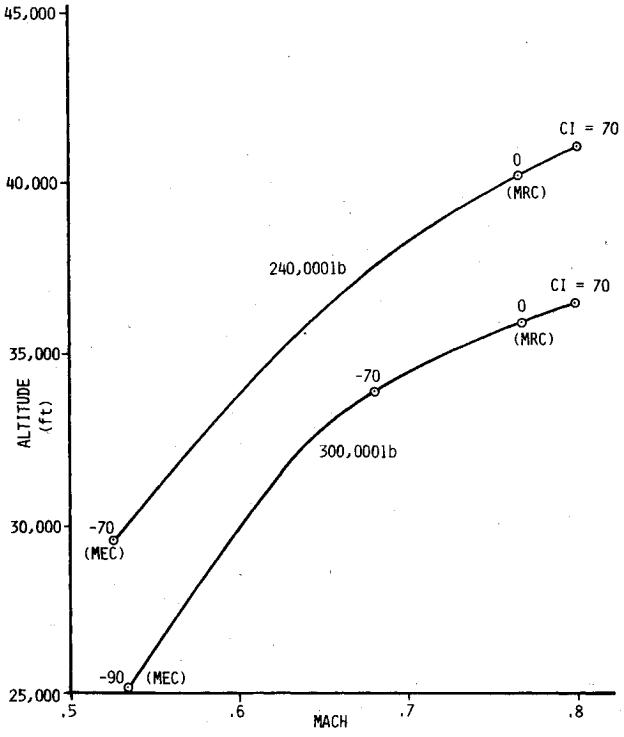


**Fig. 1 Optimal cruise altitude and Mach number (no wind).**

where the ratio to be minimized is the cruise cost function. If $\lambda_m = 0$, we get Erzberger's result for cruise cost minimization.[3]

#### Climb/Descent Cost Function

During climb/descent, we redefine the independent variable as $\tau = t/\epsilon$ for climb and $\sigma = (t - t_f)/\epsilon$ for descent such that as $\epsilon \to 0$, $\tau$, and $\sigma$ are finite over climb and descent respectively. Equation (10) is therefore transformed into

$$\min_{T,V} \left[ C_t + (C_f - \lambda_{mc}) f + \lambda_{xc} (V + V_w) + \lambda_E \frac{(V + V_w)(T - D)}{mg} \right] = 0 \qquad (14)$$

where $\lambda_{mc}$ and $\lambda_{xc}$ correspond to the values during cruise. To minimize Eq. (14), the energy adjoint

$$\lambda_E = \min_{V, D<T\le T_{\max}} - \max_{V, T_{\min}\le T<D} \left[ \frac{C_t + (C_f - \lambda_{mc}) f + \lambda_{xc} (V + V_w)}{(T - D)(V + V_w)/mg} \right]_E \qquad (15)$$

The minimization is done to get the climb solution, and the maximization to get the descent solution. The ratio in Eq. (15), to be optimized at current energy $E$, is called the climb/descent cost function, similar to Erzberger's result with $\lambda_{mc} = 0$.[3]

## Numerical Examples

Results will be presented in this paper for the Boeing 767-200 with Pratt and Whitney JT9D-7R4D engines. In all cases, the initial weight will be 240,000 lb. and the range covered will be 400 n. mi., unless specified otherwise.

Atmospheric parameters are assumed to be standard, as expressed by the 1962 International Standard Atmosphere. The cost of fuel is taken as \$0.12/lb and the optimization is performed with $\lambda_m = 0$ because it has little influence on the optimal trajectory.[4]

#### 767 Cruise Costs

Figure 1 depicts the fuel-optimal cruise altitude vs cruise Mach number for different gross weights and cost indices. The optimal solution is a cruise descent for large negative cost indices, and the flight takes place below the tropopause (36,089 ft in standard conditions). This is a surprising result. In all other cases, optimization results in a cruise climb. Tables 1 and 2 show the fuel consumption rate during cruise in pounds per second and pounds per nautical mile for two different gross weights. The fuel consumption is larger for heavier aircraft. Also, the consumption rate per unit range is minimum for maximum range cruise (MRC), while the rate per unit time is minimum for maximum endurance cruise (MEC). The case for which the minimum of the cruise cost function goes to zero is of special interest. We get[7]

$$C_t = -(C_f - \lambda_m) f_{\min}(h, T = D(m)) \qquad (16)$$

i.e., the cruise fuel flow is minimized. This is by definition maximum endurance cruise and it saves fuel to do path stretching with $\lambda_x = 0$ when the delay is sufficiently long. If $\lambda_m = 0$, Sorensen's version of maximum endurance cruise[2] is obtained. Hence, a fuel-optimal four-dimensional strategy should include a reduced speed trajectory for delay less than a critical value corresponding to $C_t$ given by Eq. (16), or a hold segment with $\lambda_x = 0$ for a longer delay.

#### Fuel-Optimal Four-Dimensional Cruise Plus Descent

A fuel-optimal controller would obtain speed and altitude commands for cruise from Eq. (13) and speed and thrust commands for descent from Eq. (15). Optimal trajectories

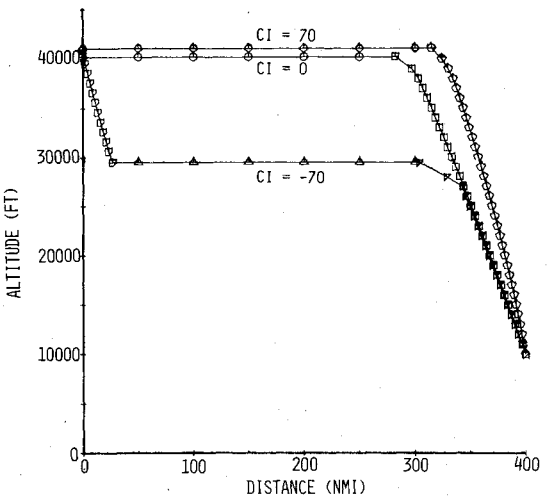


**Fig. 2 Optimal trajectories for different cost indices (no wind).**

**Table 1 Fuel consumption during cruise, (wt = 240,000 lb)**

| Cost index, \$/h | Fuel consumption rate | |
|---|---|---|
| cents/lb | lb/s | lb/n.mi. |
| +70 | 2.37 | 18.61 |
| 0 | 2.24 | 18.41 |
| −70 | 2.00 | 23.14 |

**Table 2 Fuel consumption during cruise, (wt = 300,000 lb)**

| Cost index, \$/h | Fuel consumption rate | |
|---|---|---|
| cents/lb | lb/s | lb/n.mi. |
| +70 | 2.91 | 22.95 |
| 0 | 2.79 | 22.76 |
| −70 | 2.61 | 23.91 |
| −90 | 2.54 | 28.47 |

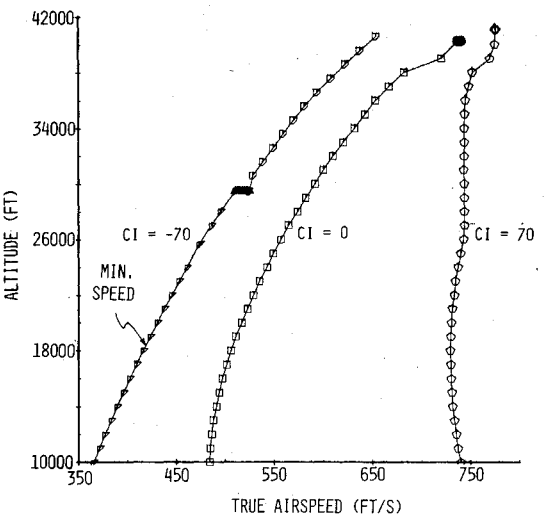


**Fig. 3 Speed-altitude plot (no wind).**

**Table 3 Convergence of $C_t$ iteration, assigned flight duration = 62.56 min, error tolerance = ±3 s (0.05 min)**

| Iteration no. | Time cost $/h | Flight duration, min |
|---|---|---|
| 1 | 0 | 59.56 |
| 2 | −571.8 | 70.34 |
| 3 | −120.5 | 61.59 |
| 4 | −176.6 | 62.47 |
| 5 | −181.0 | 62.555 |

**Table 4 Cost as a function of wind**

| Condition | Duration of flight | Fuel consumed |
|---|---|---|
| Headwind | 72.49 min | 7,324.0 lb |
| No wind | 59.56 min | 5,884.5 lb |
| Tailwind | 50.42 min | 4,913.2 lb |

over a range of 400 n. mi. are plotted in Fig. 2 for different cost indices. The bottom of descent point is taken at $h = 10{,}000$ ft. Note that the cruise altitude comes down as the cost index becomes negative. This phenomenon had not been investigated prior to this work and it requires an initial descent segment to match with the lower cruise altitude. The speed-altitude plot in Fig. 3 shows that for maximum endurance cruise, the descent takes place at minimum speed, whereas for maximum range cruise ($C_t = 0$) and positive cost indices, the descent speeds are considerably larger than minimum speed limits. For long range cruise (cost index = 70-100), the true airspeed is almost constant during descent. The thrust during descent is shown in Fig. 4. Partial thrust (greater than idle but smaller than drag) is used over a long range for negative cost indices because the descents are shallow. It should be emphasized that for numerical reasons, the thrust optimization during descent is limited to values between idle and 90% of the cruise drag. Finally, Table 3 shows a typical example of the convergence of cost of time iteration for an optimal trajectory with assigned flight duration. The tolerance level is taken as ±3 s. The iterative procedure uses the product of the first partial derivative of cost of time with respect to the flight duration and the error in the time of arrival. In the example of Table 3, it requires only five iterations to converge to the desired accuracy. In general, the number of iterations could be smaller or larger, but an average of five iterations seemed to be adequate for most problems.

#### Optimal Trajectories in the Presence of Winds

Figure 5 compares the optimal trajectories ($C_t = 0$) for headwind and tailwind with those for no wind. The terminal time is taken as free, i.e., the solution is three-dimensional fuel-optimal. The mean-wind model used is the same as that used by Menga and Erzberger[11] (Fig. 6) in their analysis. The speed-altitude plot in Fig. 7 shows an altitude, approximately 15,000 ft, below which the airspeed during descent is maximum for tailwind and minimum for headwind. This is a surprising result. The energy adjoint itself, obtained by maximizing the descent cost function, is displayed in Fig. 8 for the three cases. The cost in dollars per foot of energy is greater for headwind than for tailwind. The duration of flight and the total fuel consumption are tabulated in Table 4. Next, a delay of three minutes is introduced in each of the three cases, converting the three-dimensional problem to a four-dimensional time-controlled problem. The speed-altitude plot (Fig. 9) shows that the crossover point is conspicuously absent, i.e., the true airspeed is minimum for the tailwind all the way down to 10,000 ft. Table 5 delineates the cost of delay as a function of wind condition. The excess fuel consumption over nominal for a three-min delay is maximum for tailwind

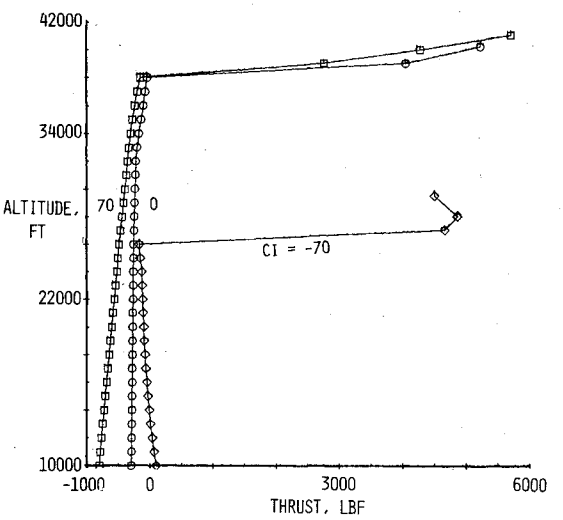


**Fig. 4 Optimal thrust during descent (no wind).**

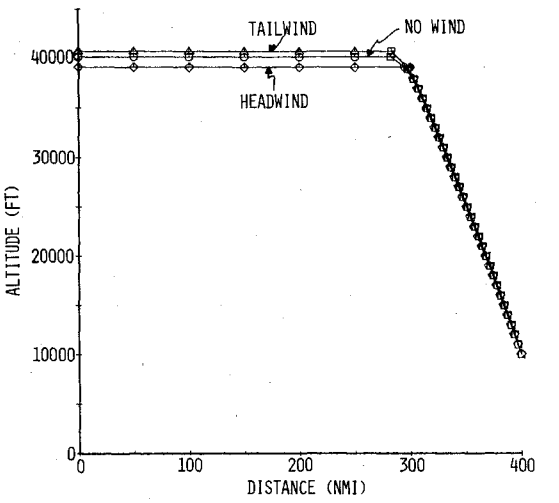


**Fig. 5 Three-dimensional optimal trajectories for different wind conditions.**

and minimum for headwind. The reason is simple. As a percentage of the nominal three-dimensional flight duration, a three-min delay is greater for tailwind than for headwind.

## Suboptimal Strategies

#### Constant Mach Number/CAS Descents Using Idle Thrust

A constant Mach number—constant Calibrated Airspeed (CAS) descent using idle thrust is analyzed and compared with the optimal strategy. The Mach number choice is equal to the optimum cruise Mach number; the CAS, a function of cost index alone, is equal to that which would be chosen by the 767 Flight Management Computer. The aircraft speed is controlled to hold Mach number constant while above the "crossover altitude," at which the chosen Mach number and CAS are equal, and constant CAS below. Two comparisons are made in Table 6. In one case, the descent is initiated from the true optimal altitude, while in the other case, descent is from the nearest Air Traffic Control (ATC) assigned altitude (39,000 ft.).

As expected, a degradation in performance is observed for descents with constant Mach number—constant CAS segments. When compared with the true optimal, the fuel consumption appears to be 1% more when the descent starts from the optimal altitude and about 2.4% more when the descent is from 39,000 ft. It should be emphasized that the

fuel spent (Table 6) is over a range of 400 n. mi. and includes both cruise and descent segments. The intention here is to show the nonoptimality of the Mach/CAS descent itself and that for a given CI, different Mach schedules are needed to descend from different cruise altitudes.

#### Constant Flight Path Angle Descents

Constant flight path angle descents are initiated from the optimal cruise altitude and the results compared with the optimal strategy. As seen in Fig. 10, a constant flight path angle descent of $-3$ deg is spatially close to the true optimal. A steeper constant flight path angle descent could require use of speedbrakes or spoilers. The descent strategy consists of optimizing speed and selecting thrust to descend along the constant flight path angle. For comparison purposes, a constant flight path angle descent of $-1$ deg is also considered. Figure 11 displays the true airspeed—altitude plot for the constant flight path angle descents and the optimal trajectory.

Even the best constant flight path angle descent is worse than the Mach/CAS descent in terms of fuel consumption, shown in Table 7. A constant flight path angle of $-3$ deg descent spends 2.1% more fuel than the true optimal, while at a shallow angle of $-1$ deg, the cost is considerably more (7.9%).

#### Effect of Wind on Constant $\gamma$ Descents

The variation of thrust during descent is shown in Fig. 12. The thrust is idle between 38,000 and 39,000 ft and, again, between 10,000 and 14,000 ft. At intermediate altitudes, however, the small thrust increment above idle could be used for groundspeed tracking in uncertain winds.

Finally, Table 8 shows the duration of flight and the fuel consumption for different wind conditions as the descent takes place at a constant flight path angle of $-3$ deg. Compare the results with those of Table 4.

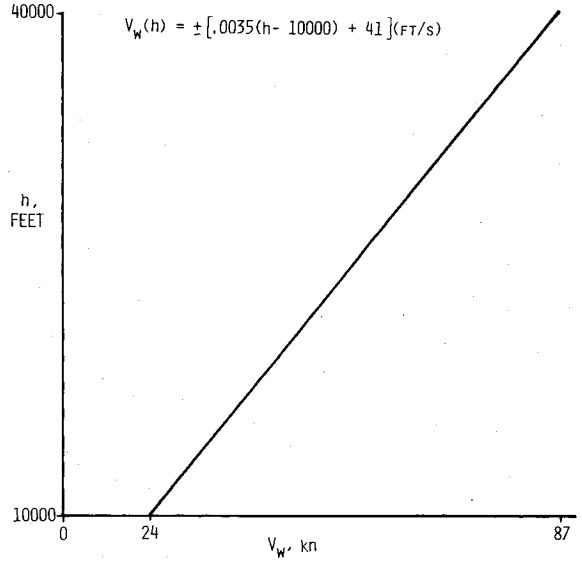


Fig. 6 Mean wind profile.

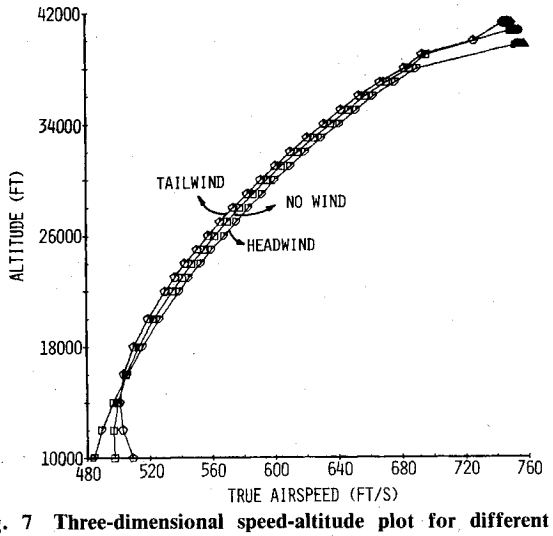


Fig. 7 Three-dimensional speed-altitude plot for different wind conditions.

Table 5 Cost of delay, delay = 3 min

| Condition | Flight duration: Three-dimensional nominal, min | Flight duration: Delayed, min | Cost index | Fuel consumed, (delayed) lb | Excess fuel used over nominal, lb |
|---|---|---|---|---|---|
| Headwind | 72.49 | 75.49 | −10.7 | 7,353.4 | 29.4 |
| No wind | 59.56 | 62.56 | −15.1 | 5,934.4 | 49.9 |
| Tailwind | 50.42 | 53.42 | −21.1 | 4,976.7 | 63.5 |

Table 6 Penalty for constant Mach/CAS descents; $C_t = 0$, no wind

| Method | Cruise altitude, ft | Total fuel spent, lb | Excess fuel used over optimal, lb |
|---|---|---|---|
| Optimal | 40,226.5 | 5,884.5 | 0 |
| Constant Mach/CAS idle thrust ($M$ = Cruise Mach = 0.76, 250K CAS) | 40,226.5 | 5,941.4 | 56.9 (0.97%) |
| Constant Mach/CAS idle-thrust ($M$ = Cruise Mach = 0.752 250K CAS) | 39,000 | 6,024.6 | 140.1 (2.4%) |

**Table 7 Cost of constant $\gamma$ descents; $C_t = 0$, no wind**

| Method | Total fuel spent, lb | Excess fuel spent over optimal, lb |
|---|---|---|
| Optimal | 5,884.5 | 0 |
| Const $\gamma = -3$ deg | 6,009.7 | 125.2 (2.1%) |
| Const $\gamma = -1$ deg | 6,352.5 | 468.0 (7.9%) |

**Table 8 Cost due to wind for constant $\gamma$ descents**

| Condition | Flight path angle, deg | Fuel consumed, lb | Duration of flight, min. |
|---|---|---|---|
| Headwind | −3 | 7,409.5 | 68.94 |
| No wind | −3 | 6,009.7 | 59.44 |
| Tailwind | −3 | 5,065.8 | 52.88 |

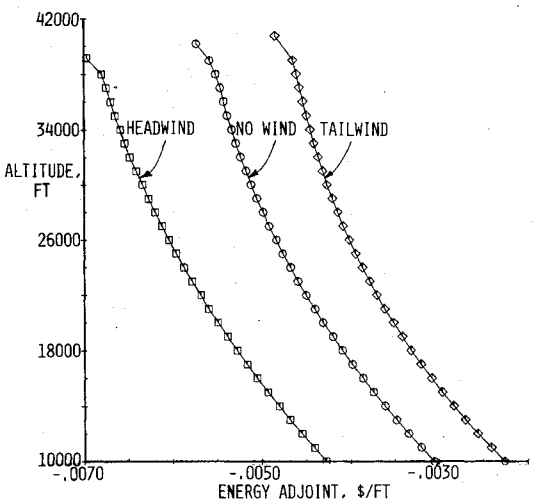


**Fig. 8 Energy adjoint for different wind conditions.**

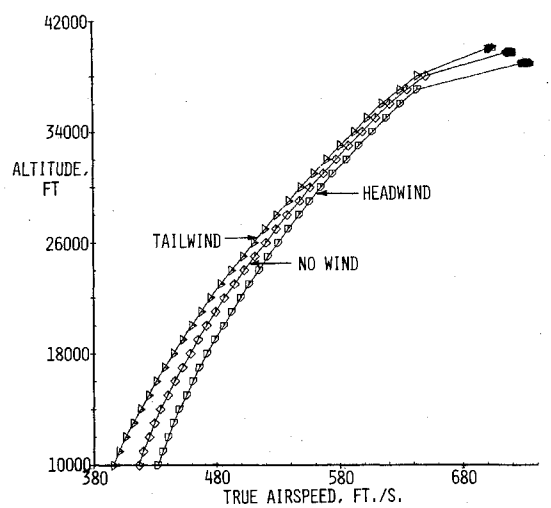


**Fig. 9 Four-dimensional speed-altitude plot for different winds.**

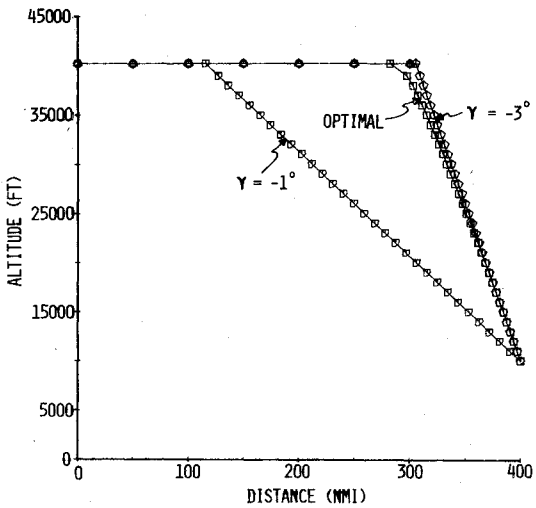


**Fig. 10 Optimal trajectories for constrant $\gamma$ descents (no wind).**

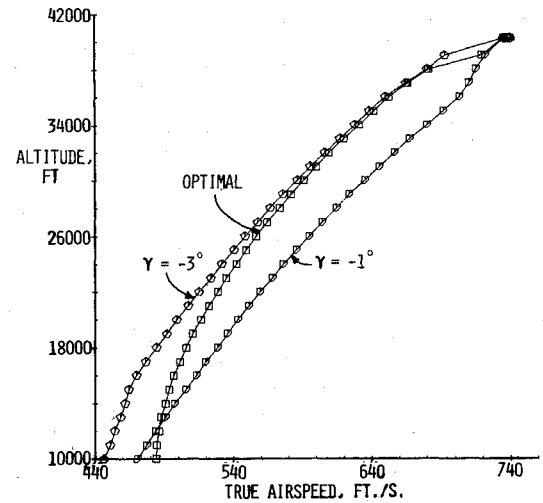


**Fig. 11 Speed-altitude plot for constant $\gamma$ descents (no wind).**

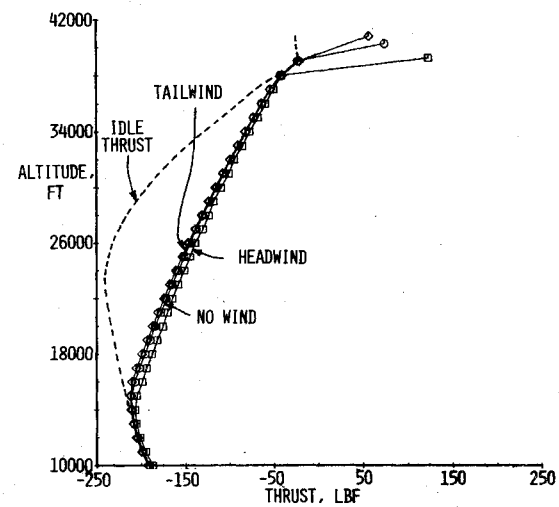


**Fig. 12 Thrust available for constant $\gamma$ descents for different winds.**

## Conclusions

1) Fuel efficient delay absorption requires a reduction in cruise altitude together with speed reduction.

2) A tailwind increases the cost of absorbing delays.

3) When descending from the optimal cruise altitude for a given cost index, it is more fuel efficient for the 767 to execute a constant Mach/CAS descent than a constant flight path angle descent.

4) For the 767 aircraft, although possibly true for other aircraft,

a) if constrained to constant flight path angle descent by Air Traffic Control (for fleet optimization and/or ease of vectoring), the steepest descent possible without drag device deployment should be selected,

b) the true fuel-optimal cruise segment consists of a cruise descent at larger negative values of cost of time and occurs below the tropopause. In all other cases, the optimal solution is a cruise climb.

## References

[1]Chakravarty, A. and Vagners, J., "Application of Singular Perturbation Theory to Onboard Aircraft Trajectory Optimization," AIAA Paper 81-0019, Jan. 1981.

[2]Sorensen, J.A. and Waters, M.H., "Airborne Method to Minimize Fuel with Fixed Time-of-Arrival Constraints," *Journal of Guidance and Control,* Vol. 4, May-June 1981, pp. 348-349.

[3]Erzberger, H. and Lee, H., "Constrained Optimum Trajectories with Specified Range," *Journal of Guidance and Control,* Vol. 3, Jan.-Feb. 1980, pp. 78-85.

[4]Burrows, J.W., "Fuel-Optimal Aircraft Trajectories with Fixed Arrival Times," *Journal of Guidance and Control,* Vol. 6, Jan.-Feb. 1983, pp. 14-19.

[5]Calise, A.J., "Singular Perturbation Techniques for On-Line Optimal Flight-Path Control," *Journal of Guidance and Control,* Vol. 4, July-Aug. 1981, pp. 398-405.

[6]Mehra, R.K., Washburn, R.B., Sajan, S., and Carroll, J.V., "A Study of the Application of Singular Perturbation Theory," NASA CR-3167, Aug. 1979.

[7]Chakravarty, A. and Vagners, J., "Development of 4-D Time-Controlled Guidance Laws Using Singular Perturbation Methodology," 1982 American Control Conference, Arlington, Va., June 1982, pp 1107-1108.

[8]Chakravarty, A. and Vagners, J., "4-D Aircraft Flight Path Management in Real Time," 1983 American Control Conference, San Francisco, Calif., June 1983, pp. 794-795.

[9]Kevorkian, J. and Cole, J.D., *Perturbation Methods in Applied Mathematics,* Springer-Verlag, New York, 1981, pp 7-16.

[10]Bryson, A.E. and Ho, Y.C., *Applied Optimal Control,* John Wiley and Sons, New York, 1975, pp. 108-109.

[11]Menga, G. and Erzberger, H., "Time-Controlled Descent Guidance in Uncertain Winds," *Journal of Guidance and Control,* Vol. 1, March-April 1978, pp. 123-129.